RESEARCH ARTICLE SUMMARY

HOMININ GENETICS

Recurrent gene flow between Neanderthals and modern humans over the past 200,000 years

Liming Li, Troy J. Comi, Rob F. Bierman, Joshua M. Akey*

INTRODUCTION: For much of modern human history, we were only one of several different groups of hominins that existed. Studies of ancient and modern DNA have shown that admixture occurred multiple times among different hominin lineages, including between the ancestors of modern humans and Neanderthals. A number of methods have been developed to identify Neanderthal-introgressed sequences in the DNA of modern humans, which have provided insight into how admixture with Neanderthals shaped the biology and evolution of modern human genomes. Although gene flow from an early modern human population to Neanderthals has been described, the consequences of admixture on the Neanderthal genome have received comparatively less attention.

RATIONALE: A better understanding of how admixture with modern humans influenced patterns of Neanderthal genomic variation may provide insights into hominin evolutionary history. For example, DNA sequences inherited from modern human ancestors in Neanderthals can be used to test hypotheses on frequency, magnitude, and timing of admixture and the population genetics characteristics of Neanderthals. Introgressed modern human sequences in Neanderthals can also be used to refine estimates of Neanderthal ancestry in contemporary individuals. We developed a simple framework to investigate introgressed human sequences in Neanderthals that is predicated on the expectation that sequences inherited from modern human ancestors would be, on average, more genetically diverse and would result in local increases in heterozygosity across the Neanderthal genome.

RESULTS: We first used a method referred to as IBDmix to identify introgressed Neanderthal sequences in 2000 modern humans sequenced by the 1000 Genomes Project. We found that sequences identified by IBDmix as Neanderthal in African individuals from the 1000 Genomes Project are significantly enriched in regions of high heterozygosity in the Neanderthal genome, whereas no such enrichment is observed with sequences detected as introgressed in non-African individuals. We show that these patterns are caused by gene flow from modern humans to Neanderthals and estimate that the Vindija and Altai Neanderthal genomes have 53.9 Mb (2.5%) and 80.0 Mb (3.7%) of human-introgressed sequences, respectively. We leverage human-introgressed sequences in Neanderthals to revise estimates of the amount of Neanderthal-introgressed sequences in modern humans. Additionally, we show that human-introgressed sequences cause Neanderthal population size to be overestimated and that accounting for their effects decrease estimates of Neanderthal population size by ~20%. Finally, we found evidence for two distinct epochs of human gene flow into Neanderthals.

CONCLUSION: Our results provide insights into the history of admixture between modern humans and Neanderthals, show that gene flow had substantial impacts on patterns of modern human and Neanderthal genomic variation, and show that accounting for human-introgressed sequences in Neanderthals enables more-accurate inferences of admixture and its consequences in both Neanderthals and modern humans. More generally, the smaller estimated population size and inferred admixture dynamics are consistent with a Neanderthal population that was decreasing in size over time and was ultimately being absorbed into the modern human gene pool. ■

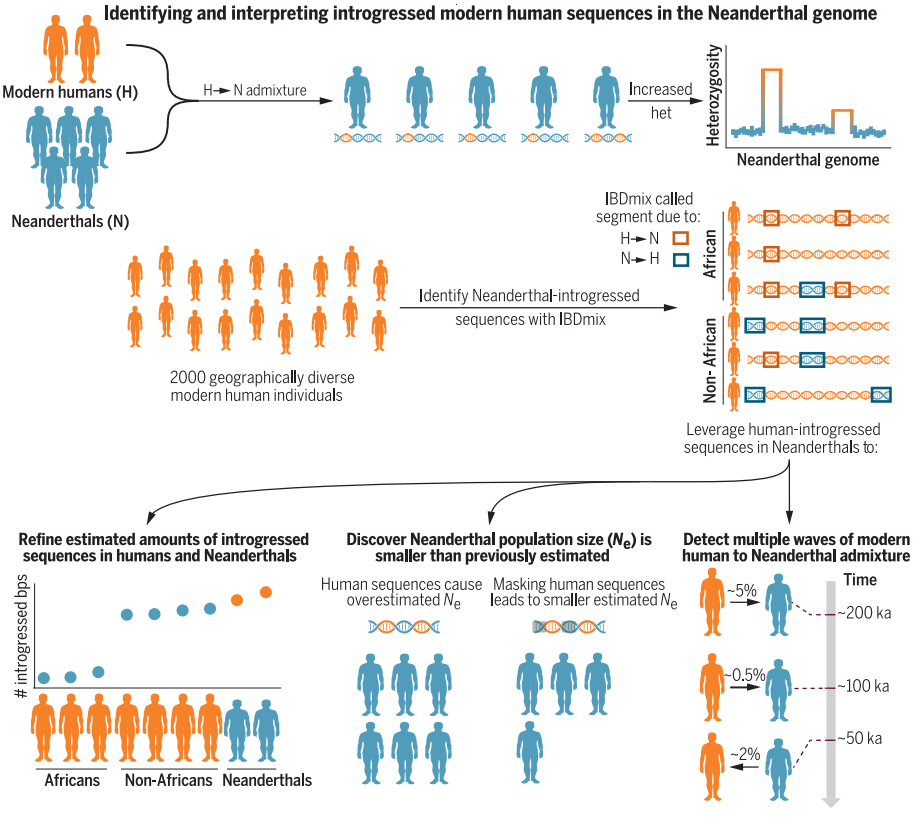

Detecting modern human–to-Neanderthal gene flow (H→N) and its consequences. Modern human–to-Neanderthal admixture causes a local increase in heterozygosity in the Neanderthal genome, a characteristic that enabled approaches to quantify and detect introgressed sequences. We leveraged modern human–introgressed sequences in the Neanderthal genome to refine estimates of Neanderthal ancestry in contemporary humans by decomposing IBDmix-detected segments into those attributable to human-to-Neanderthal (H→N) versus Neanderthal-to-human (N→H) gene flow in 2000 modern human individuals. We also used modern human–introgressed sequences to discover that Neanderthals had a smaller effective population size (N_e) than previously estimated and that a second wave of modern human–to-Neanderthal gene flow occurred ~100 to 120 thousand years ago (ka). bps, base pairs.

The list of author affiliations is available in the full article online.
*Corresponding author. Email: jakey@princeton.edu
Cite this article as L. Li *et al.*, *Science* **385**, eadi1768 (2024).
DOI: 10.1126/science.adi1768

READ THE FULL ARTICLE AT
https://doi.org/10.1126/science.adi1768

RESEARCH ARTICLE

HOMININ GENETICS

Recurrent gene flow between Neanderthals and modern humans over the past 200,000 years

Liming Li[1,2], Troy J. Comi[2], Rob F. Bierman[2], Joshua M. Akey[2]*

Although it is well known that the ancestors of modern humans and Neanderthals admixed, the effects of gene flow on the Neanderthal genome are not well understood. We develop methods to estimate the amount of human-introgressed sequences in Neanderthals and apply it to whole-genome sequence data from 2000 modern humans and three Neanderthals. We estimate that Neanderthals have 2.5 to 3.7% human ancestry, and we leverage human-introgressed sequences in Neanderthals to revise estimates of Neanderthal ancestry in modern humans, show that Neanderthal population sizes were significantly smaller than previously estimated, and identify two distinct waves of modern human gene flow into Neanderthals. Our data provide insights into the genetic legacy of recurrent gene flow between modern humans and Neanderthals.

Studies of ancient DNA have shown that admixture among modern humans (*Homo sapiens*), Neanderthals, and Denisovans has played a prominent role in hominin evolutionary history (*1*). Although genetic data from Neanderthal and Denisovan individuals continue to accumulate (*2*–*10*), inferences of gene flow among hominin lineages have largely focused on high-coverage, whole-genome sequence (WGS) data from three Neanderthals and one Denisovan (*3*–*6*). The Vindija (*4*) and Chagyrskaya (*5*) Neanderthals were excavated from the Vindija cave in Croatia and the Chagyrskaya cave in the Altai Mountains, respectively, whereas the Altai Neanderthal (also referred to as Denisova 5) (*3*) and the Denisovan hominin (also named Denisova 3) (*6*) were both excavated from the Denisova Cave in the Altai Mountains. These genomes combined with WGS data from thousands of modern humans have revealed a network of interactions—including gene flow—between modern humans and Neanderthals (*2*, *3*, *11*), between modern humans and two distinct Denisovan populations (*12*), and between Neanderthals and Denisovans (*3*, *13*), including an F1 hybrid who had a Neanderthal mother and Denisovan father (*10*). In modern humans, non-African individuals derive ~2% of their genome from Neanderthal ancestors (*2*), and individuals of Melanesian and Australian aboriginal ancestry can trace an additional 2 to 5% of their genome to Denisovan ancestors, with the highest levels in certain Philippine groups (*14*).

In addition to estimates of admixture proportions, numerous approaches have been developed to identify the specific DNA sequences in the genomes of modern humans that were inherited from Neanderthals and Denisovans (*15*–*17*). The resulting catalogs of introgressed sequences have enabled their functional, phenotypic, and evolutionary consequences to be studied (*18*–*23*). For example, analyses of Neanderthal-introgressed sequences in modern humans have shown that they were targets of both purifying and positive selection (*24*–*26*), have facilitated the development of more-refined admixture models (*24*, *27*–*30*), and have enabled insights into the phenotypic legacy of admixture (*23*).

In contrast to the detailed studies of how admixture with Neanderthals affected the genomes of modern humans, comparatively little is known about the consequences that admixture had on the Neanderthal genome. Several studies have shown evidence of modern human ancestry in the Neanderthal genome (*31*–*33*) as a result of admixture that predates the out-of-Africa dispersal of ~60 thousand years ago (ka) (*11*, *34*), to which contemporary non-Africans can trace the majority of their ancestry (*35*–*38*). Thus, admixture between modern humans and Neanderthals has occurred at least twice, with one admixture resulting in modern human–to-Neanderthal (H→N) gene flow ~250 to 200 ka and the other admixture resulting in Neanderthal-to–modern human (N→H) gene flow ~60 to 50 ka (*39*) (Fig. 1A). The signal of modern human–to-Neanderthal gene flow was initially detected in the Altai Neanderthal (*31*) but was also subsequently found in the Vindija (*32*), which suggests that admixture occurred before the divergence of these two lineages (Fig. 1A).

The observation of modern human ancestry in the Neanderthal genome due to H→N gene flow raises important questions about the dynamics and significance of introgressed modern human sequence in the Neanderthal genome. For example, Neanderthals had a substantially lower effective population size (denoted as N_e) and, thus, less genetic diversity compared with modern humans (*3*–*5*). Therefore, modern human–introgressed sequences in Neanderthals may affect inferences of Neanderthal genetic diversity and population genetics parameters. Additionally, the number, timing, and magnitude of admixture events that led to modern human ancestry in Neanderthals is not well defined. Finally, the presence of modern human–introgressed sequences in Neanderthals may confound inferences about how much Neanderthal ancestry exists in modern human individuals. To address these questions and better delimit the admixture history and its impact on both modern humans and Neanderthals, we developed a methodological framework to better understand the magnitude and consequences of modern human–to-Neanderthal gene flow.

Expected characteristics of human-introgressed sequences in Neanderthals

Our approach for investigating modern human–to-Neanderthal gene flow is predicated on two observations made in previous studies of hominin admixture. First, our framework takes advantage of the well-known differences in N_e between modern humans and Neanderthals (*3*–*5*). Second, our approach derives power from the fact that both H→N and N→H gene flow make substantial contributions to the signal of Neanderthal-introgressed sequences identified in African individuals (*33*), whereas the signal of Neanderthal-introgressed sequences detected in non-African individuals is primarily the result of N→H admixture (*2*, *33*).

Given these observations, we hypothesized that introgressed modern human sequences in Neanderthal genomes would result in local increases in levels of heterozygosity (Fig. 1, B and C) given the larger N_e of modern humans compared with that of Neanderthals. If true, we would expect regions of high heterozygosity in the Neanderthal genome to overlap sequences identified as Neanderthal in African individuals more often compared with sequences identified as Neanderthal in non-African individuals (Fig. 1B). We would further expect that when regions of high heterozygosity in the Neanderthal genome are masked, the amount of detected introgressed sequence would decrease more in Africans compared with non-Africans (because the signal from H→N admixture is attenuated, which preferentially affects African individuals; Fig. 1B). Below, we evaluate these predicted features using empirical data.

Regions of high heterozygosity in Neanderthal genomes are enriched for introgressed modern human sequences

To assess the relationship between Neanderthal heterozygosity and the probability of calling

[1]Department of Medical Genetics and Developmental Biology, School of Medicine, The Key Laboratory of Developmental Genes and Human Diseases, Ministry of Education, Southeast University, Nanjing 210009, China. [2]The Lewis-Sigler Institute for Integrative Genomics, Princeton University, Princeton, NJ 08540, USA.
*Corresponding author. Email: jakey@princeton.edu

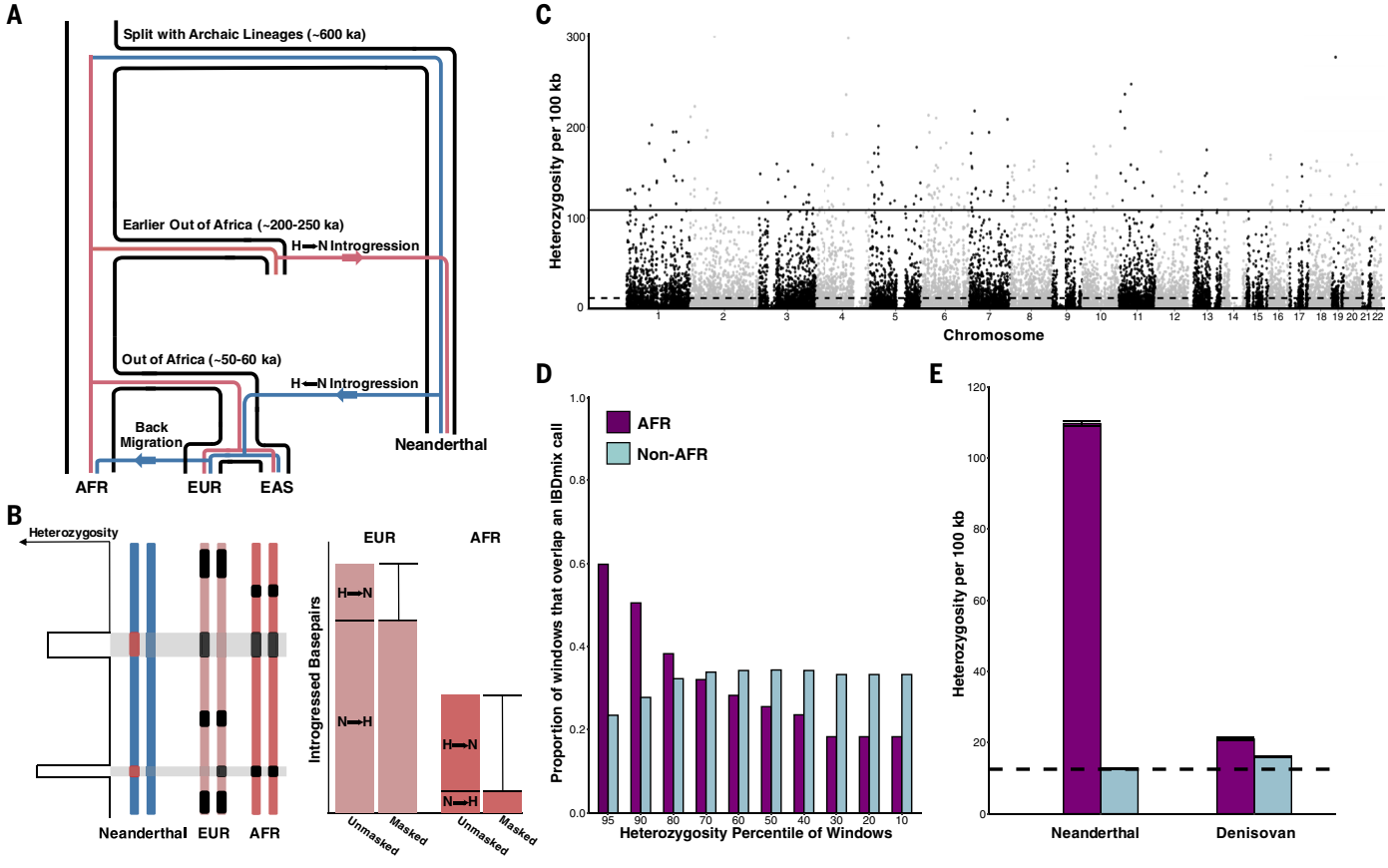

Fig. 1. Neanderthal-introgressed sequences identified in African individuals are associated with regions of high heterozygosity in the Neanderthal genome. (**A**) Schematic of modern human–to-Neanderthal (H⟶N) and Neanderthal-to–modern human (N⟶H) gene flow. Red and blue lines represent modern human and Neanderthal lineages, respectively. AFR, EUR, and EAS denote African, European, and East Asian, respectively. (**B**) Schematic showing how H⟶N admixture can lead to regions of high heterozygosity in the Neanderthal genome and calls of introgressed Neanderthal sequence in modern humans. Two Neanderthal, AFR, and EUR chromosomes are shown. Red segments in Neanderthal chromosomes denote modern human–introgressed sequences due to H⟶N gene flow. Black segments represent IBDmix-called introgressed Neanderthal sequences in modern humans due to a mixture of H⟶N and N⟶H gene flow. H⟶N admixture can result in local increases of heterozygosity, whereas N⟶H admixture does not. The bar plot shows the amount of introgressed sequence identified in EUR and AFR samples when the entire genome is analyzed (unmasked) or when loci in the human genome that overlap high-heterozygosity regions in the Neanderthal genome (gray rectangles) are removed from the analysis (masked). (**C**) Genome-wide distribution of heterozygosity calculated in nonoverlapping 100-kb windows across the Altai Neanderthal genome. Solid and dashed lines represent the 99th percentile and average heterozygosity, respectively. (**D**) Proportion of windows in the Altai Neanderthal genome that overlap AFR (purple) and non-AFR (light blue) calls of introgressed Neanderthal sequences as a function of heterozygosity in the Neanderthal genome. The *x* axis represents the percentile of heterozygosity for analyzed windows. Heterozygosity of windows decreases from left to right. (**E**) Heterozygosity in regions of the Altai Neanderthal and Denisovan genomes that overlap IBDmix calls of introgressed Neanderthal sequence in Africans and non-Africans. The dashed line represents the genome-wide average heterozygosity of Altai.

introgressed Neanderthal sequences in Africans and non-Africans, we applied IBDmix (*33*) to 2000 individuals from the 1000 Genomes Project (*40*). IBDmix detects introgressed sequences by identifying segments in a test genome that are shared identical by descent with an archaic reference genome. To mitigate false positives, a minimum segment size threshold is used, which we previously specified in units of physical distance (*33*). In this work, we extended IBDmix to also allow segment sizes to be measured in units of genetic distance, which results in a lower false discovery rate (FDR) while maintaining the same power compared with physical distance–based thresholds (*41*) (fig. S1). Using a minimum segment size threshold of 0.05 centimorgans (cM), we identified 92.4, 85.5, and 84.3 gigabases (Gb) of introgressed Neanderthal sequence across all 2000 individuals using the Vindija Neanderthal (*4*), Altai Neanderthal (*3*), and Chagyrskaya Neanderthal (*5*) as the archaic reference genome, respectively (table S1).

IBDmix calls in African individuals were significantly enriched at locations of the human genome that overlap regions of high heterozygosity in the Neanderthal genome compared with those in non-African individuals [$P < 10^{-6}$; (*41*)] (Fig. 1D). For example, 60% of windows in the top fifth percentile of high-heterozygosity regions in the Altai genome overlapped calls of Neanderthal-introgressed sequence in Africans compared with only 23% of windows in non-Africans (Fig. 1D). Similar patterns were observed with the Vindija and Chagyrskaya genomes (fig. S2). Furthermore, Neanderthal heterozygosity in regions that overlap calls of introgressed sequence in Africans is 8.6 times as high relative to Neanderthal heterozygosity in regions that overlap introgressed sequence in non-Africans (Fig. 1E). As a control, we compared levels of heterozygosity in the same regions of the Denisovan genome and only observed a 1.3-fold difference in heterozygosity between Africans and non-Africans (Fig. 1E). In addition, Kuhlwilm *et al.* (*31*) have reported 162 regions of the Altai Neanderthal genome that had elevated heterozygosity and were

putatively introgressed from modern humans, of which 130 overlap our high-heterozygosity regions, which is significantly more than expected by chance [$P = 1.63 \times 10^{-24}$; (*41*)]. Collectively, these observations demonstrate that regions of high heterozygosity in the Neanderthal genome are enriched for modern human–introgressed sequences.

Decomposing IBDmix calls into their component sources

Genomic segments that IBDmix detects as Neanderthal introgressed are potentially a mixture of sequences derived from both H→N and N→H gene flow. Thus, to specifically investigate the characteristics of modern human–to-Neanderthal gene flow, it is necessary to distinguish between these two component sources. To this end, we evaluated whether the summary statistics R_{Ind} and R_{Pop} (*41*) could distinguish between IBDmix calls of introgressed sequence attributable to H→N or N→H gene flow. R_{Ind} is the ratio of the average number of introgressed base pairs per individual called by IBDmix in Africans relative to Europeans, and R_{Pop} is the ratio of the number of base pairs of the reference modern human genome covered by one or more IBDmix calls in Africans relative to that in Europeans (*41*, *42*). We estimated R_{Ind} and R_{Pop} using each of the five African populations and Europeans from the 1000 Genomes Project (*40*) and evaluated their relationship with levels of heterozygosity in the Neanderthal genome (*41*). Both R_{Ind} and R_{Pop} are higher for LWK (Luhya in Webuye, Kenya) and GWD (Gambian in Western Division, The Gambia) compared with MSL (Mende in Sierra Leone), YRI (Yoruba in Ibadan, Nigeria), and ESN (Esan in Nigeria), which suggests that they have higher amounts of introgressed Neanderthal sequence (Fig. 2A). Despite the quantitative differences in R_{Ind} and R_{Pop} among African populations, they all qualitatively show the same pattern as a function of heterozygosity in the Neanderthal genome. In particular, R_{Ind} and R_{Pop} decrease precipitously when masking the top 10% of windows with the highest heterozygosity in the Neanderthal genome before converging to stable values as progressively more of the Neanderthal genome is masked (Fig. 2A and figs. S3 and S4). The initial decrease observed for R_{Ind} and R_{Pop} when the most heterozygous regions in the Neanderthal genome are masked indicates that less introgressed Neanderthal sequence is identified in African relative to non-African individuals.

To help interpret the empirical patterns of R_{Ind} and R_{Pop}, we performed coalescent simulations of a model with H→N gene flow, a model of N→H gene flow with migration back to Africa, and a joint model with both H→N and N→H gene flow (*41*) (Fig. 2B and fig. S5). For each admixture model, we simulated 15 Mb of sequence in 503 Europeans, 108 Africans, and 3 Neanderthals; identified introgressed

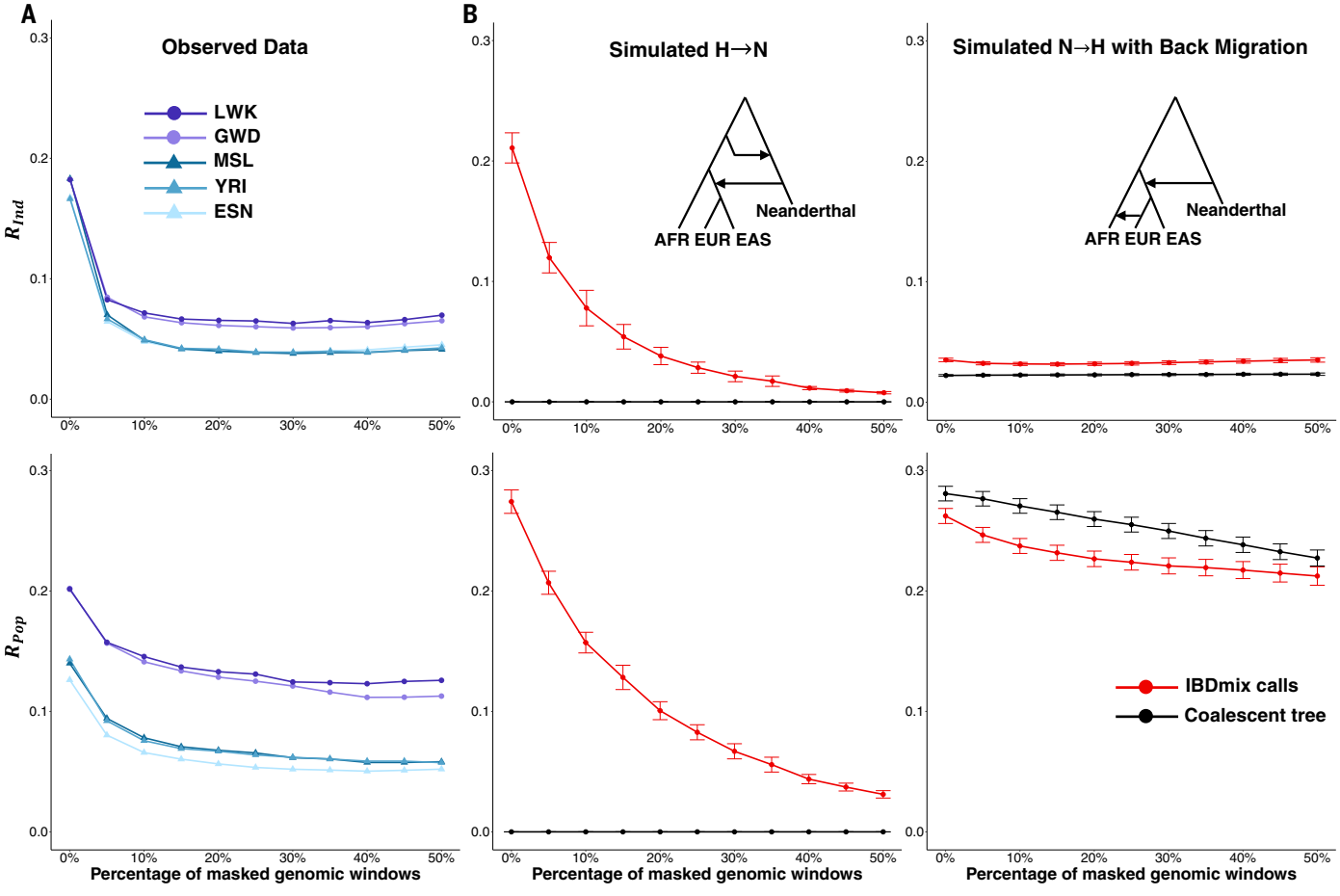

Fig. 2. R_{Ind} and R_{Pop} can distinguish between admixture models. We show R_{Ind} and R_{Pop} as a function of heterozygosity in the Altai Neanderthal genome. The *x* axis represents the percentage of high-heterozygosity windows in the Neanderthal genome that are masked when identifying Neanderthal-introgressed sequences with IBDmix. Thus, heterozygosity decreases from left to right. (**A**) We estimated R_{Ind} and R_{Pop} using Europeans and each of the five African populations from the 1000 Genomes Project, including Luhya in Webuye, Kenya (LWK); Gambian in Western Division, The Gambia (GWD); Esan in Nigeria (ESN); Mende in Sierra Leone (MSL); and Yoruba in Ibadan, Nigeria (YRI). (**B**) Estimates of R_{Ind} and R_{Pop} in the simulated data. The red and black lines represent values of R_{Ind} and R_{Pop} that were calculated from Neanderthal-introgressed sequences identified by IBDmix and those obtained directly from the coalescent tree, respectively.

sequences with IBDmix; and calculated R_{Ind} and R_{Pop} as a function of heterozygosity in the simulated Neanderthal genome. In the H→N admixture model, all Neanderthal-introgressed sequences detected by IBDmix in Africans are due to modern human gene flow into Neanderthals (Fig. 2B). By contrast, in the N→H model, all Neanderthal-introgressed sequences in Africans identified by IBDmix are the result of gene flow from Neanderthals into non-Africans followed by the migration of individuals carrying Neanderthal sequence back to Africa (Fig. 2B). In the joint model, all Neanderthal-introgressed sequences detected by IBDmix in Africans are due to both H→N and N→H gene flow (fig. S5).

In the H→N model, R_{Ind} and R_{Pop} decrease as a function of heterozygosity in the Neanderthal genome and tend toward zero (Fig. 2B). In the N→H model with back migration, R_{Ind} and R_{Pop} behaved much differently and were relatively flat as a function of Neanderthal heterozygosity (Fig. 2B). In the joint model, R_{Ind} and R_{Pop} decrease as a function of heterozygosity in the Neanderthal genome and tend toward those estimated using Neanderthal-introgressed sequences obtained from the coalescent tree (fig. S5). The differences in patterns of R_{Ind} and R_{Pop} between admixture models are robust to the presence of false positives in the IBDmix call set (fig. S5). Overall, the simulations demonstrate that both H→N and N→H with back migration contribute to the observed patterns of R_{Ind} and R_{Pop} in the empirical data. Specifically, H→N gene flow is necessary to account for the higher observed values of R_{Ind} and R_{Pop} without masking and their rapid decline when the most heterozygous windows of the Neanderthal genome are masked. Similarly, N→H admixture with back migration explains the low but nonzero values of R_{Ind} and R_{Pop} in the empirical data when windows with high heterozygosity in the Neanderthal genome are masked. In summary, these data provide additional evidence that introgressed modern human sequences contribute to regions of high heterozygosity in the Neanderthal genome and that the relationship between R_{Ind} and R_{Pop} and levels of Neanderthal heterozygosity can be leveraged to quantitatively decompose the proportion of introgressed sequences in modern humans due to H→N and N→H gene flow.

Estimating the proportion of modern human ancestry in Neanderthals

We next developed an approach to estimate the amount of modern human ancestry in Neanderthals that is based on the relationship between R_{Pop} and Neanderthal heterozygosity (fig. S4) and an orthogonal statistic to detect Neanderthal-introgressed sequences in non-Africans known as S^* (*4*, *24*, *27*, *41*) (fig. S6). Using this method, we estimate the Vindija and Altai genomes contain 53.9 and 80.0 Mb of modern human–introgressed sequence, respectively (table S2), and these estimates are robust to the choice of which African population is used to calculate R_{Pop} (fig. S4 and table S2). Accounting for the fraction of masked genomic regions (*41*), this corresponds to ~2.5 and 3.7% modern human ancestry in Vindija and Altai, respectively, which is higher than the estimated amount of Neanderthal ancestry in present-day modern humans (*24*, *27*). We performed a gene ontology (GO) analysis to test whether human-introgressed sequences were enriched for particular GO biological process and molecular function terms (*41*). We identified five terms that were significantly enriched (FDR ≤ 0.05) after correcting for multiple hypothesis tests (table S3). Two of the enriched GO terms, metal ion transmembrane transporter activity (FDR = 7.16×10^{-3}) and glutamate receptor signaling pathway (FDR = 7.81×10^{-3}), are composed of numerous genes that influence central nervous system biology, neurotransmitter uptake and metabolism, and other neuronal processes, mutations in several of which have been associated with intellectual disability [*CACNG2*, *GRIA1*, and *SLC6A11* (*43*–*45*)], autism [*GRIN2B* (*46*)], and other neurodevelopmental disorders [*GRIK2* and *GRM7* (*47*, *48*)]. However, additional work is necessary to better interpret the biological significance of the observed GO enrichment results.

Revising estimates of Neanderthal ancestry in modern humans

The total amount of IBDmix-detected Neanderthal sequence can be decomposed into amounts attributable to N→H and H→N gene flow using the same methodological framework to estimate the amount of modern human–introgressed sequences in Neanderthals (*41*). In these analyses, however, we used R_{Ind} instead of R_{Pop} because our goal is to estimate the amount of introgressed sequence per individual, which is more straightforward to calculate with R_{Ind} (*41*) (fig. S3). To evaluate our approach, we performed simulations and found that it is robust to several potential confounding variables, including recombination rate heterogeneity, Neanderthal effective population size, and the time and magnitude of H→N gene flow (figs. S7 to S13).

When using Vindija as the Neanderthal reference genome, IBDmix identified a total of 62.3, 60.1, and 55.8 Mb of Neanderthal sequence per individual in East Asians, South Asians, and Europeans, respectively (table S4). The percentage (and amount) of total IBDmix-identified Neanderthal sequence attributable to N→H gene flow is 91.1% (56.8 Mb), 92.3% (55.5 Mb), and 91.8% (51.2Mb) in East Asians, South Asians, and Europeans, respectively (Fig. 3 and table S4). In African populations, the total amount of IBDmix-detected Neanderthal sequence per individual ranged from 6.2 Mb in YRI to 8.0 Mb in LWK (table S4). The percentage (and amount) of IBDmix-identified Neanderthal sequence due to N→H gene flow ranged from a low of 25.6% (1.8 Mb) in MSL to a high of 39.4% (2.9 Mb) in GWD (Fig. 3 and table S4). These results are broadly consistent when using Altai as the reference genome (Fig. 3), except the estimated percentage of total Neanderthal sequence called by IBDmix that is attributable to H→N gene flow increased modestly (see the legend of table S4 for an explanation of this observation). Collectively, these data show that Neanderthal-introgressed sequences in Africans and non-Africans are influenced by both H→N and N→H gene flow but their relative contributions differ among populations.

Neanderthals had significantly smaller population sizes than previously thought

The presence of human-introgressed sequences in Neanderthal genomes could potentially influence estimates of their N_e. To test this hypothesis, we compared estimates of the long-term N_e of Neanderthal lineages before and after correcting for modern human–to-Neanderthal admixture. Without accounting for H→N gene flow (*41*), the estimated long-term N_e of Altai, Chagyrskaya, and Vindija were 3369 [95% confidence interval (CI), 3036 to 3520], 2964 (95% CI, 2765 to 3148), and 3408 (95% CI, 3209 to 3554) individuals, respectively (Fig. 4A and table S5), which is similar to previous estimates (*4*, *5*). After removing human-introgressed sequences by masking regions of the Neanderthal genome that overlapped African IBDmix calls (*41*), the estimated long-term N_e significantly ($P < 0.05$) decreased in all three Neanderthal lineages. Specifically, the estimated N_e in Altai, Chagyrskaya, and Vindija decreased to 2484 (95% CI, 2223 to 2639), 2379 (95% CI, 2181 to 2569), and 2807 (95% CI, 2622 to 2959) individuals, respectively (Fig. 4A and table S5). This constitutes a reduction in the long-term N_e of 26.3% in Altai, 19.7% in Chagyrskaya, and 17.5% in Vindija (table S5).

To assess the robustness of these results, we first estimated N_e in Denisovans with and without masking genomic regions that carry modern human–introgressed sequences in Neanderthals. As expected, the Denisovan estimates of N_e differ by only 1.92% (3824 versus 3899; $P > 0.05$; table S5). We confirmed by coalescent simulations that the observed amount of human to Neanderthal gene flow can inflate estimates of N_e in Neanderthals by amounts commensurate with the empirical data (*41*). We also performed analyses to show that the smaller estimates of N_e when accounting for H→N gene flow are robust to heterogeneity in locus-specific mutation rates and false positive IBDmix calls in African individuals (*41*).

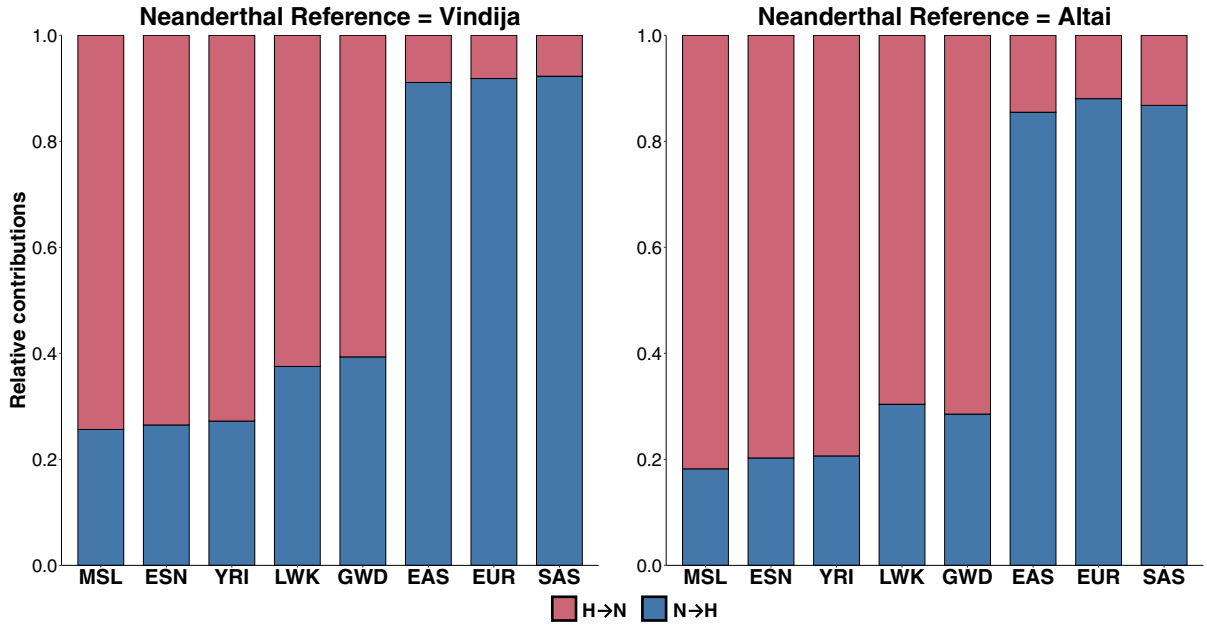

Fig. 3. Decomposing the signal of Neanderthal ancestry in modern human populations. Each bar shows the average proportion of Neanderthal-introgressed sequence per individual due to H→N and N→H gene flow across eight geographically diverse populations. Results are shown when using the Vindija (left) or Altai (right) Neanderthal as the archaic reference genome.

Additionally, we used PSMC (pairwise sequentially Markovian coalescent) (*41*) to estimate N_e, which also shows that estimates of N_e over time are smaller when accounting for modern human–introgressed sequences (Fig. 4B). Conversely, PSMC estimates of Denisovan and Mbuti N_e (*41*) did not change with and without removing regions that carry modern human–introgressed sequence in Neanderthals (Fig. 4B and fig. S14).

Previous estimates of N_e were roughly the same in Altai and Vindija (*4*, *5*). However, when accounting for modern human–introgressed sequences, we found that the N_e of Vindija is 13% higher than that of Altai (table S5), which suggests that Altai had a smaller N_e after it split with other Neanderthal lineages. We performed simulations to estimate the N_e of the Altai lineage after it split from the common ancestor of the Vindija and Chagyrskaya lineages and the N_e of the Chagyrskaya lineage after it split from the common ancestor of the Vindija lineage. We estimate that the N_e of the Altai and Chagyrskaya lineages are 45 and 27%, respectively, the size relative to the Vindija lineage (Fig. 4C). These estimates are similar when assuming different times and magnitude of H→N gene flow (fig. S15).

These data show that Neanderthals had smaller and more variable population sizes among lineages than previously thought. The ~20% lower estimate of long-term N_e has important implications for the cost of introgression to modern humans because it potentially allowed more deleterious mutations to accumulate in Neanderthals that were subsequently inherited by the ancestors of predominantly non-African populations (*26*, *49*, *50*).

Evidence for two distinct pulses of modern human–to-Neanderthal gene flow

Although previous studies have found evidence for gene flow from modern humans to Neanderthals (*31*–*33*), they assumed a single period of admixture, and more-complex models have not been explored. We used our revised estimates of N_e in Neanderthals to evaluate single- versus multiple-pulse models of H→N gene flow. We first tested whether we could confirm a previous inference of gene flow from early modern humans into Neanderthals between 200 and 300 ka (*32*). We found that our data are most consistent with models where the H→N admixture fraction was 5% and the time of admixture was 200 ka or where the admixture fraction was 10% and the time of admixture was 250 ka, but the data are less consistent with a model where the admixture fraction is 10% and admixture occurred 200 ka (*41*) (fig. S3B and fig. S16).

We leveraged the temporal variation of the Altai [age = 122 ka (*4*)], Chagyrskaya [age = 80 ka (*5*)], and Vindija [age = 52 ka (*4*)] Neanderthals to develop an approach for evaluating admixture models with an additional wave of modern human–to-Neanderthal gene flow. Specifically, we asked whether Vindija, Chagyrskaya, or both Vindija and Chagyrskaya received an additional wave of H→N admixture relative to Altai. One- versus two-pulse admixture models were formally assessed by approximate Bayesian computation (ABC) (*41*), which has been used in a wide variety of inference problems in population genetics (*51*–*53*). In ABC, summary statistics are used to assess the fit between observed and simulated data, and this information provides the basis to calculate approximate posterior probabilities of distinct models and the approximate posterior distribution of model parameters (*53*–*55*).

To implement an ABC method for evaluating admixture models, we first developed 10 summary statistics that capture a broad set of potential features in the data that may be informative for distinguishing between one- and two-pulse models of H→N gene flow (table S6). We evaluated informativeness through coalescent simulations in which each summary statistic was calculated in a one-pulse model and 20 two-pulse models parameterized by the time $T_{H\rightarrow N}$ and magnitude $\alpha_{H\rightarrow N}$ of the second admixture (*41*). For each two-pulse model, we calculated the power of the summary statistics to distinguish between one- and two-pulse admixture models and Cohen's *D*, which is a measure of effect size (fig. S17 and table S7). Each summary statistic exhibited high power (≥80%) and modest-to-large effect sizes for at least part of the parameter space considered (table S7), and therefore, we retained all 10 summary statistics in the ABC model.

We next evaluated the power of our ABC framework through extensive coalescent simulations (*41*). Briefly, for each replicate, we simulated WGS data in 1120 individuals from 10 distinct two-pulse models, which we treated as "real data" in an ABC analysis (*41*). We then

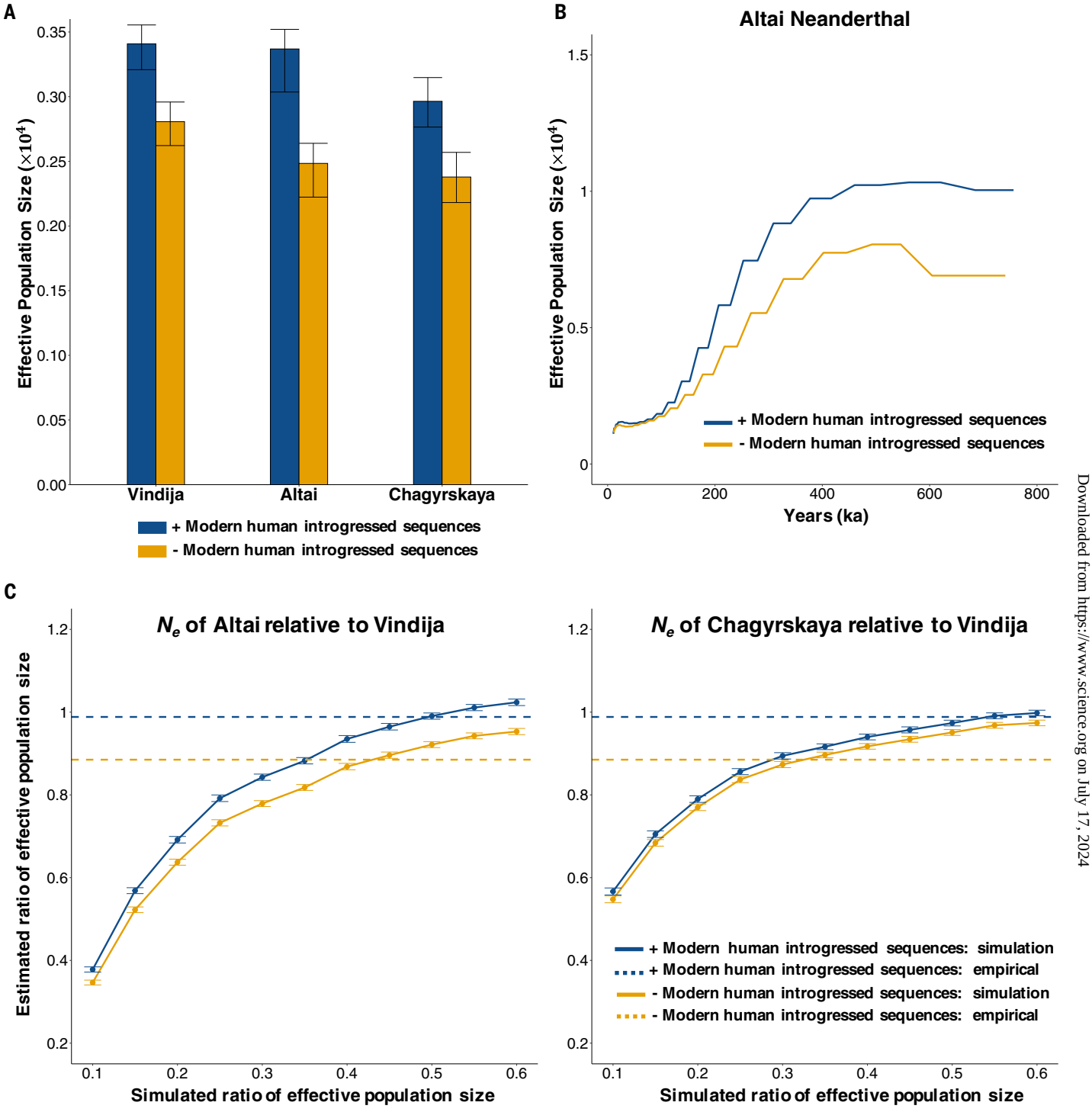

Fig. 4. Modern human–introgressed sequences in Neanderthals lead to biased estimates of effective population size N_e. Estimates of N_e when modern human–introgressed sequences are masked (− modern human–introgressed sequences) or are not masked (+ modern human–introgressed sequences). (**A**) Estimates of N_e and its 95% CI for Vindija, Altai, and Chagyrskaya. (**B**) PSMC estimates of N_e throughout time for the Altai Neanderthal. (**C**) We simulated models that varied the ratio of N_e for Altai relative to Vindija (left) and the ratio of N_e for Chagyrskaya relative to Vindija (right). We estimated the Altai-Vindija and Chagyrskaya-Vindija ratios of N_e under each model (solid lines) and compared them with the empirical ratios (dashed lines).

calculated a Bayes factor (BF), which we defined as the ratio of approximate posterior probabilities between the two-pulse and one-pulse models, and estimated power as the fraction of the total simulation replicates where the BF ≥ t (multiple thresholds, t, were considered) and correctly selected the two-pulse over the one-pulse model (*41*). Our ABC method exhibited high power (≥80%) across a broad range of two-pulse models, with some models exhibiting BFs ≥ 50 (table S8). Furthermore, the posterior modes of $\alpha_{H\to N}$ and $T_{H\to N}$ almost

always coincided with the true parameter value (tables S9 and S10). Power was lower when the magnitude of the second pulse was small and occurred more distantly in the past ($\alpha_{H\rightarrow N}$ = 0.25% and $T_{H\rightarrow N} \geq 120$ ka; table S8). We also estimated the false positive rate (FPR) by performing ABC analyses on replicates simulated from the one-pulse model (*41*), and, as expected, the FPR decreases as the BF threshold increases and with BF ≥ 5, the FPR is $<2 \times 10^{-4}$ (table S11).

We applied our ABC method to the empirical data to test the hypothesis of an additional wave of H→N gene flow in the Vindija and Chagyrskaya lineages (*41*). In the ABC analysis, we compared the observed data with simulated data from a one-pulse and 40 distinct two-pulse models parameterized by $T_{H\rightarrow N}$ = [60 ka, 80 ka, …, 140 ka] and $\alpha_{H\rightarrow N}$ = [0.25%, 0.50%, …, 2%]. Note, the range of $T_{H\rightarrow N}$ considered covers the upper and lower bounds of plausible times for a second H→N pulse of gene flow, given that the Vindija and Chagyrskaya lineages split from the Altai lineage ~140 ka (*4*) and that the Vindija and Chagyrskaya fossils were estimated to be ~52 ka (*4*) and 80 ka (*5*), respectively. Both Vindija and Chagyrskaya exhibited significant evidence for a second pulse of H→N gene flow (table S12). Specifically, Vindija and Chagyrskaya had BFs ≥ 20 for 12 and 5 two-pulse models, respectively (table S12). The most supported two-pulse model for Vindija (BF = 123) was for an additional pulse of H→N gene flow that occurred $T_{H\rightarrow N}$ = 100 ka with an admixture fraction of $\alpha_{H\rightarrow N}$ = 0.5% (table S12). Similarly, the most supported two-pulse model for Chagyrskaya (BF = 67) was for an additional pulse of H→N gene flow that occurred $T_{H\rightarrow N}$ = 120 ka with an admixture fraction of $\alpha_{H\rightarrow N}$ = 0.5% (table S12). These were also the values of $T_{H\rightarrow N}$ and $\alpha_{H\rightarrow N}$ with the highest approximate posterior probabilities for Vindija and Chagyrskaya (Fig. 5A). To ensure that these results were robust, we repeated the ABC analysis using transversions only when calculating *D* statistics (*1*) and found that our estimates of $T_{H\rightarrow N}$ and $\alpha_{H\rightarrow N}$ did not change (*41*) (fig. S18). These estimates were similar to those obtained when using a neural network correction implemented in the "abc" package (*41*). Overall, the ABC results are broadly concordant between Vindija and Chagyrskaya (Fig. 5A and table S12) and are consistent with a second pulse of modern human–to-Neanderthal gene flow ~120 to 100 ka of substantially smaller magnitude relative to the first wave of H→N admixture (Fig. 5B).

Discussion

Advances in the sequencing and analysis of modern and ancient genomes have enabled remarkable insights into hominin evolutionary history and the relationship between modern and extinct humans (*11*). For example, analyses of WGS data from Neanderthals and modern humans revealed the now well-characterized admixture that occurred between these lineages ~60 to 50 ka (*39*), which resulted in the introgression of Neanderthal sequences into modern human genomes (*2*). In this work, we provide insights into the long admixture history and dynamics of gene flow between modern humans and Neanderthals. Our data, along with previous studies (*31*–*33*), show that recurrent episodes of gene flow, beginning ~250 to 200 ka, affected the genomes and biology of both modern humans and Neanderthals.

As predicted by Chen *et al.* (*33*), we find that both H→N and N→H gene flow contribute to IBDmix calls of Neanderthal-introgressed sequence in the 1000 Genomes Project populations, with the relative contribution varying among populations. In the non-African populations studied, N→H gene flow accounts for ~90% of detected introgressed sequences, whereas in the African populations studied, H→N gene flow explained 61 to 82% of the signal depending on the specific population and Neanderthal reference genome used. Similarly, Harris *et al.* (*56*) recently used IBDmix to identify Neanderthal-introgressed sequences in 12 sub-Saharan African populations. Consistent with Chen *et al.* (*33*) and our current study, they found that H→N and N→H gene flow contributed to IBDmix-detected sequences for four of the populations that they studied. However, for the other eight sub-Saharan populations, they estimated that H→N gene flow accounted for all, or nearly all, of the IBDmix-detected signal of Neanderthal ancestry (*56*). Thus, some sub-Saharan African populations may not have any Neanderthal-introgressed sequence. We note that IBDmix is sensitive to allele frequency estimates (*33*), and the populations that they studied had relatively small sample sizes and potential genetic structure (*56*), which may reduce the power of IBDmix to detect introgressed sequences (*33*). Nonetheless, it seems clear that although all contemporary human populations harbor the signal of a shared historical dispersal that led to H→N gene flow, the amount of introgressed segments attributable to N→H admixture is unevenly distributed across the African continent. Additional studies of genetically and geographically diverse African populations will be necessary to more precisely delimit the distribution of Neanderthal-introgressed sequences across Africa. Such data may provide insights into historical patterns of admixture among African populations and the timing and routes of migration throughout Africa. Furthermore, even small amounts of Neanderthal ancestry discovered in future studies of diverse African populations, if robustly inferred from large enough sample

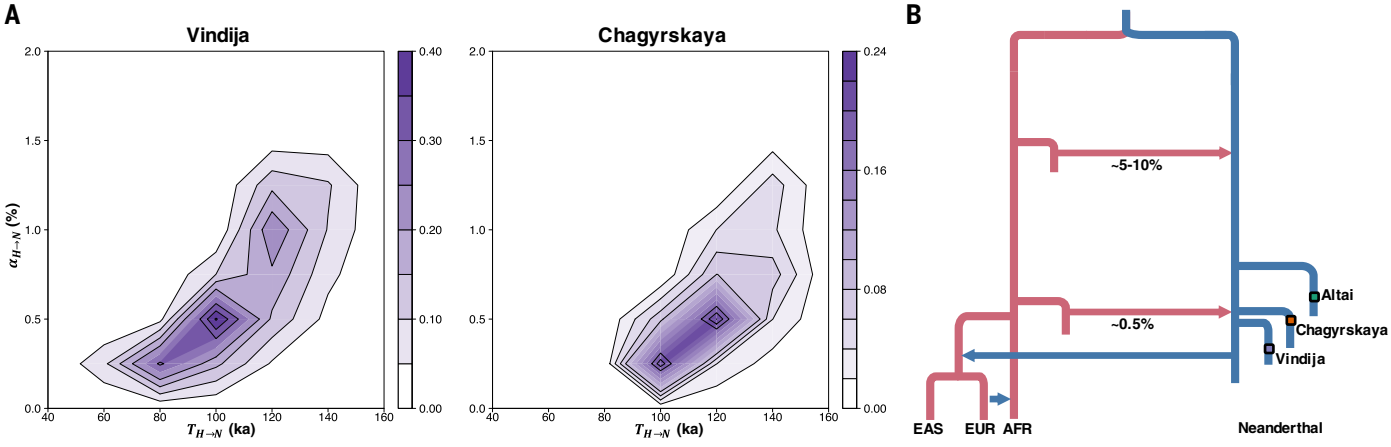

Fig. 5. Multiple waves of modern human–to-Neanderthal gene flow. (**A**) Contour plots showing the posterior distribution of the admixture proportion ($\alpha_{H\rightarrow N}$) and time of admixture ($T_{H\rightarrow N}$) estimated using ABC for the Vindija (left) and Chagyrskaya (right) Neanderthal. (**B**) Schematic illustration showing the recurrent admixture events between modern humans and Neanderthals, including the two waves of H→N gene flow.

sizes, would have important implications for understanding African evolutionary history.

The initial wave of H→N admixture occurred ~250 to 200 ka and represents an early dispersal of modern humans from Africa. This early dispersal is broadly consistent with the fossil record both within and outside of Africa. For example, the first morphological features of anatomically modern humans emerged in Africa ~300 ka (*57*–*60*), and fully anatomically modern fossil remains discovered in southern Ethiopia date to a minimum age of 233 ka (*61*). Thus, early to fully anatomically modern humans existed in this time frame. Additionally, the fossil record shows that early modern humans had dispersed out of Africa by at least ~200 ka (*62*–*64*). Of particular relevance is the Apidima 1 fossil from the Apidima Cave in southern Greece that dates to ~210 ka (*62*), which shows that these early out-of-Africa diasporas were not confined to the Levant (*63*) but in some cases covered substantial distances. Although it is difficult to speculate on where the first wave of H→N admixture occurred, sequencing more Neanderthal genomes that span additional points in space and time would be fruitful in addressing this question. Finally, it remains to be seen whether these early migrations from Africa were able to extend into the range of Denisovans (*14*), but future studies that look for evidence of modern human–to-Denisovan gene flow may be useful in identifying previously unknown out-of-Africa dispersals and providing insight into the timing and ranges that they covered.

We also found evidence for an additional pulse of modern human–to-Neanderthal gene flow ~120 to 100 ka. This timing is consistent with the presence of the Nile-Sinai land bridge between 130 and 96 ka (*65*) and fossil and archeological data showing that modern humans reached the Levant (*66*) and Arabian Peninsula in this time frame (*67*, *68*). We caution that inference of complex demographic models is challenging, and additional models could also be compatible with the data. However, our results, coupled with other archaeological (*66*, *69*), geographic (*65*, *67*, *68*), and genetic (*31*–*33*, *70*–*72*) evidence, demonstrate that although contemporary non-African populations can trace much of their ancestry to a single out-of-Africa dispersal 50 to 60 ka (*35*–*38*), these early, effectively extinct dispersals of modern humans out of Africa nonetheless played an important role in hominin evolutionary history.

More broadly, the quantitative patterns of recurrent gene flow between modern humans and Neanderthals that we describe over the course of ~200 ka offer a perspective on factors possibly related to the disappearance of Neanderthals. Specifically, we show that the magnitude of H→N gene flow decreased through time, from 5 to 10% at 250 to 200 ka, to 0.5% at 120 to 100 ka, to 0% for late Neanderthals who lived between 47 and 39 ka (*8*). Conversely, as H→N gene flow ceased, numerous examples of N→H admixture began to appear. These include N→H gene flow ~60 to 50 ka with an initial Neanderthal admixture proportion as high as 10% (*26*, *49*), possible additional waves of N→H admixture in specific modern human populations such as East Asians (*11*, *17*), and ancient DNA from several early modern humans who lived ~39 to 45 ka that show evidence of more-recent N→H gene flow (*73*, *74*). This asymmetric admixture pattern, where gene flow is primarily detected in one direction, initially from H→N but then from N→H, suggests a Neanderthal population that was decreasing in size over time, eventually reaching a point where it was not large enough to absorb modern humans into their gene pool. At this time, gene flow reverses direction, and the one-way flow of Neanderthal genes into modern humans may have contributed to the extinction of Neanderthals (*75*). Specifically, the assimilation of Neanderthals into modern human populations (*75*–*77*) as they spread throughout Eurasia would have effectively increased the size of modern human populations while simultaneously decreasing the size of an already at-risk Neanderthal population. Our finding that the effective population size of Neanderthals was likely even smaller than previously estimated would only hasten the assimilation process, and the replacement of the Y chromosome (*71*) and mitochondrial DNA (*72*) in late Neanderthals by modern humans may have marked an irrevocable path toward the disappearance of one of the few remaining hominin lineages that coexisted with modern humans.

Materials and methods summary

We analyzed WGS data from 2000 unrelated individuals generated by the 1000 Genomes Project (*40*) (table S1). Additionally, we analyzed the following high-coverage archaic genomes: Altai Neanderthal (*3*), Vindija Neanderthal (*4*), Chagyrskaya Neanderthal (*5*), and Denisovan (*6*). We downloaded genotype data in variant call format (VCF) for Altai, Vindija, and Denisovan from http://cdna.eva.mpg.de/neandertal/Vindija/VCF/ and for Chagyrskaya from http://cdna.eva.mpg.de/neandertal/Chagyrskaya/VCF/.

We improved the IBDmix algorithm (*33*) such that it has a lower false positive rate compared with our previous implementation (fig. S1) and used it to identify introgressed Neanderthal sequences in the 1000 Genomes Project individuals. We generated IBDmix call sets separately using Altai, Vindija, and Chagyrskaya as the archaic reference genome. We then evaluated the relationship between heterozygosity in the genomes of Altai, Vindija, and Chagyrskaya and IBDmix calls of introgressed sequence in African and non-African individuals from the 1000 Genomes Project. We calculated two summary statistics, R_{Ind} and R_{Pop} (*41*), in empirical and simulated data to help interpret the correlation observed between genomic locations of IBDmix calls in African individuals and regions of high heterozygosity in the Neanderthal genomes.

We developed an approach to estimate the amount of modern human–introgressed sequence in Neanderthals and Neanderthal-introgressed sequence in modern humans using R_{Pop}, R_{Ind}, IBDmix, and S^* (*4*, *41*). Briefly, IBDmix is sensitive to both H→N and N→H gene flow, whereas S^* is only well powered to detect N→H admixture. Thus, we can leverage the different characteristics of IBDmix and S^* to formulate an approach to distinguish between H→N and N→H gene flow (*41*). We evaluated our approach by performing extensive coalescent simulations and showing that estimates were robust to a number of potential confounding factors (*41*).

We investigated whether modern human–introgressed sequences influenced estimates of the effective population size, N_e, of Neanderthals. We used heterozygosity to estimate the long-term N_e of Altai, Vindija, and Chagyrskaya with and without masking IBDmix calls of introgressed sequences made in African individuals. We also estimated N_e of Neanderthals as a function of time using PSMC (*41*) with and without masking IBDmix calls of introgressed sequences made in African individuals. In addition, we estimated N_e of Altai and Chagyrskaya lineages after they split from the introgressing and Vindija lineages. We performed coalescent simulations to evaluate the quantitative relationship between the amount of modern human–to-Neanderthal gene flow and magnitude of bias in estimates of N_e (*41*).

To test the hypothesis of additional waves of modern human–to-Neanderthal admixture, we performed ABC. Specifically, we tested whether there was evidence for a second pulse of gene flow from modern humans specifically to Neanderthal lineages after they split from Altai. We evaluated the power of 10 summary statistics to detect a second wave of modern human–to-Neanderthal admixture through coalescent simulations. We also used coalescent simulations to evaluate the power and false positive rate of ABC to identify a second pulse of gene flow conditional on using these 10 summary statistics and other aspects of the empirical data (*41*). ABC was performed on the observed data to determine whether a model of two waves of modern human–to-Neanderthal admixture better explained the data compared with a single pulse of admixture and to estimate the posterior distribution of the timing ($T_{H\to N}$) and magnitude ($\alpha_{H\to N}$) of the second pulse.

REFERENCES AND NOTES

1. H. Zeberg, M. Jakobsson, S. Pääbo, The genetic changes that shaped Neandertals, Denisovans, and modern humans. *Cell* **187**, 1047–1058 (2024). doi: 10.1016/j.cell.2023.12.029; pmid: 38367615
2. R. E. Green *et al*., A draft sequence of the Neandertal genome. *Science* **328**, 710–722 (2010). doi: 10.1126/science.1188021; pmid: 20448178
3. K. Prüfer *et al*., The complete genome sequence of a Neanderthal from the Altai Mountains. *Nature* **505**, 43–49 (2014). doi: 10.1038/nature12886; pmid: 24352235
4. K. Prüfer *et al*., A high-coverage Neandertal genome from Vindija Cave in Croatia. *Science* **358**, 655–658 (2017). doi: 10.1126/science.aao1887; pmid: 28982794
5. F. Mafessoni *et al*., A high-coverage Neandertal genome from Chagyrskaya cave. *Proc. Natl. Acad. Sci. U.S.A.* **117**, 15132–15136 (2020). doi: 10.1073/pnas.2004944117; pmid: 32546518
6. M. Meyer *et al*., A high-coverage genome sequence from an archaic Denisovan individual. *Science* **338**, 222–226 (2012). doi: 10.1126/science.1224344; pmid: 22936568
7. L. Skov *et al*., Genetic insights into the social organization of Neanderthals. *Nature* **610**, 519–525 (2022). doi: 10.1038/s41586-022-05283-y; pmid: 36261548
8. M. Hajdinjak *et al*., Reconstructing the genetic history of late Neanderthals. *Nature* **555**, 652–656 (2018). doi: 10.1038/nature26151; pmid: 29562232
9. L. Bokelmann *et al*., A genetic analysis of the Gibraltar Neanderthals. *Proc. Natl. Acad. Sci. U.S.A.* **116**, 15610–15615 (2019). doi: 10.1073/pnas.1903984116; pmid: 31308224
10. V. Slon *et al*., The genome of the offspring of a Neanderthal mother and a Denisovan father. *Nature* **561**, 113–116 (2018). doi: 10.1038/s41586-018-0455-x; pmid: 30135579
11. R. Nielsen *et al*., Tracing the peopling of the world through genomics. *Nature* **541**, 302–310 (2017). doi: 10.1038/nature21347; pmid: 28102248
12. S. R. Browning, B. L. Browning, Y. Zhou, S. Tucci, J. M. Akey, Analysis of Human Sequence Data Reveals Two Pulses of Archaic Denisovan Admixture. *Cell* **173**, 53–61.e9 (2018). doi: 10.1016/j.cell.2018.02.031; pmid: 29551270
13. B. M. Peter, 100,000 years of gene flow between Neandertals and Denisovans in the Altai mountains. BioRxiv 2020.03.13.990523 (2020); doi: 10.1101/2020.03.13.990523
14. S. Peyrégne, V. Slon, J. Kelso, More than a decade of genetic research on the Denisovans. *Nat. Rev. Genet.* **25**, 83–103 (2024). doi: 10.1038/s41576-023-00643-4; pmid: 37723347
15. F. Racimo, S. Sankararaman, R. Nielsen, E. Huerta-Sánchez, Evidence for archaic adaptive introgression in humans. *Nat. Rev. Genet.* **16**, 359–371 (2015). doi: 10.1038/nrg3936; pmid: 25963373
16. S. Sankararaman, Methods for detecting introgressed archaic sequences. *Curr. Opin. Genet. Dev.* **62**, 85–90 (2020). doi: 10.1016/j.gde.2020.05.026; pmid: 32717667
17. A. B. Wolf, J. M. Akey, Outstanding questions in the study of archaic hominin admixture. *PLOS Genet.* **14**, e1007349 (2018). doi: 10.1371/journal.pgen.1007349; pmid: 29852022
18. M. Dannemann, K. Prüfer, J. Kelso, Functional implications of Neandertal introgression in modern humans. *Genome Biol.* **18**, 61 (2017). doi: 10.1186/s13059-017-1181-7; pmid: 28366169
19. R. M. Gittelman *et al*., Archaic Hominin Admixture Facilitated Adaptation to Out-of-Africa Environments. *Curr. Biol.* **26**, 3375–3382 (2016). doi: 10.1016/j.cub.2016.10.041; pmid: 27839976
20. R. C. McCoy, J. Wakefield, J. M. Akey, Impacts of Neanderthal-Introgressed Sequences on the Landscape of Human Gene Expression. *Cell* **168**, 916–927.e12 (2017). doi: 10.1016/j.cell.2017.01.038; pmid: 28235201
21. C. N. Simonti *et al*., The phenotypic legacy of admixture between modern humans and Neandertals. *Science* **351**, 737–741 (2016). doi: 10.1126/science.aad2149; pmid: 26912863
22. H. Zeberg, S. Pääbo, The major genetic risk factor for severe COVID-19 is inherited from Neanderthals. *Nature* **587**, 610–612 (2020). doi: 10.1038/s41586-020-2818-3; pmid: 32998156
23. P. F. Reilly, A. Tjahjadi, S. L. Miller, J. M. Akey, S. Tucci, The contribution of Neanderthal introgression to modern human traits. *Curr. Biol.* **32**, R970–R983 (2022). doi: 10.1016/j.cub.2022.08.027; pmid: 36167050
24. B. Vernot, J. M. Akey, Resurrecting surviving Neandertal lineages from modern human genomes. *Science* **343**, 1017–1021 (2014). doi: 10.1126/science.1245938; pmid: 24476670
25. S. Sankararaman *et al*., The genomic landscape of Neanderthal ancestry in present-day humans. *Nature* **507**, 354–357 (2014). doi: 10.1038/nature12961; pmid: 24476815
26. M. Petr, S. Pääbo, J. Kelso, B. Vernot, Limits of long-term selection against Neandertal introgression. *Proc. Natl. Acad. Sci. U.S.A.* **116**, 1639–1644 (2019). doi: 10.1073/pnas.1814338116; pmid: 30647110
27. B. Vernot *et al*., Excavating Neandertal and Denisovan DNA from the genomes of Melanesian individuals. *Science* **352**, 235–239 (2016). doi: 10.1126/science.aad9416; pmid: 26989198
28. F. A. Villanea, J. G. Schraiber, Multiple episodes of interbreeding between Neanderthal and modern humans. *Nat. Ecol. Evol.* **3**, 39–44 (2019). doi: 10.1038/s41559-018-0735-8; pmid: 30478305
29. B. Y. Kim, K. E. Lohmueller, Selection and reduced population size cannot explain higher amounts of Neandertal ancestry in East Asian than in European human populations. *Am. J. Hum. Genet.* **96**, 454–461 (2015). doi: 10.1016/j.ajhg.2014.12.029; pmid: 25683122
30. C. S. Quilodrán, J. Rio, A. Tsoupas, M. Currat, Past human expansions shaped the spatial pattern of Neanderthal ancestry. *Sci. Adv.* **9**, eadg9817 (2023). doi: 10.1126/sciadv.adg9817; pmid: 37851812
31. M. Kuhlwilm *et al*., Ancient gene flow from early modern humans into Eastern Neanderthals. *Nature* **530**, 429–433 (2016). doi: 10.1038/nature16544; pmid: 26886800
32. M. J. Hubisz, A. L. Williams, A. Siepel, Mapping gene flow between ancient hominins through demography-aware inference of the ancestral recombination graph. *PLOS Genet.* **16**, e1008895 (2020). doi: 10.1371/journal.pgen.1008895; pmid: 32760067
33. L. Chen, A. B. Wolf, W. Fu, L. Li, J. M. Akey, Identifying and Interpreting Apparent Neanderthal Ancestry in African Individuals. *Cell* **180**, 677–687.e16 (2020). doi: 10.1016/j.cell.2020.01.012; pmid: 32004458
34. A. Bergström, C. Stringer, M. Hajdinjak, E. M. L. Scerri, P. Skoglund, Origins of modern human ancestry. *Nature* **590**, 229–237 (2021). doi: 10.1038/s41586-021-03244-5; pmid: 33568824
35. S. Tucci, J. M. Akey, A map of human wanderlust. *Nature* **538**, 179–180 (2016). doi: 10.1038/nature19472; pmid: 27654916
36. A. S. Malaspinas *et al*., A genomic history of Aboriginal Australia. *Nature* **538**, 207–214 (2016). doi: 10.1038/nature18299; pmid: 27654914
37. S. Mallick *et al*., The Simons Genome Diversity Project: 300 genomes from 142 diverse populations. *Nature* **538**, 201–206 (2016). doi: 10.1038/nature18964; pmid: 27654912
38. L. Pagani *et al*., Genomic analyses inform on migration events during the peopling of Eurasia. *Nature* **538**, 238–242 (2016). doi: 10.1038/nature19792; pmid: 27654910
39. S. Sankararaman, N. Patterson, H. Li, S. Pääbo, D. Reich, The date of interbreeding between Neandertals and modern humans. *PLOS Genet.* **8**, e1002947 (2012). doi: 10.1371/journal.pgen.1002947; pmid: 23055938
40. 1000 Genomes Project Consortium, A global reference for human genetic variation. *Nature* **526**, 68–74 (2015). doi: 10.1038/nature15393; pmid: 26432245
41. See the supplementary materials.
42. B. Vernot, J. M. Akey, Complex history of admixture between modern humans and Neandertals. *Am. J. Hum. Genet.* **96**, 448–453 (2015). doi: 10.1016/j.ajhg.2015.01.006; pmid: 25683119
43. F. F. Hamdan *et al*., Excess of de novo deleterious mutations in genes associated with glutamatergic systems in nonsyndromic intellectual disability. *Am. J. Hum. Genet.* **88**, 306–316 (2011). doi: 10.1016/j.ajhg.2011.02.001; pmid: 21376300
44. V. Ismail *et al*., Identification and functional evaluation of *GRIA1* missense and truncation variants in individuals with ID: An emerging neurodevelopmental syndrome. *Am. J. Hum. Genet.* **109**, 1217–1241 (2022). doi: 10.1016/j.ajhg.2022.05.009; pmid: 35675825
45. W. Y. Son *et al*., Gaba transporter *SLC6A11* gene polymorphism associated with tardive dyskinesia. *Nord. J. Psychiatry* **68**, 123–128 (2014). doi: 10.3109/08039488.2013.780260; pmid: 23795861
46. H. A. F. Stessman *et al*., Targeted sequencing identifies 91 neurodevelopmental-disorder risk genes with autism and developmental-disability biases. *Nat. Genet.* **49**, 515–526 (2017). doi: 10.1038/ng.3792; pmid: 28191889
47. J. R. Stolz *et al*., Clustered mutations in the *GRIK2* kainate receptor subunit gene underlie diverse neurodevelopmental disorders. *Am. J. Hum. Genet.* **108**, 1692–1709 (2021). doi: 10.1016/j.ajhg.2021.07.007; pmid: 34375587
48. M. S. Reuter *et al*., Diagnostic Yield and Novel Candidate Genes by Exome Sequencing in 152 Consanguineous Families With Neurodevelopmental Disorders. *JAMA Psychiatry* **74**, 293–299 (2017). doi: 10.1001/jamapsychiatry.2016.3798; pmid: 28097321
49. K. Harris, R. Nielsen, The Genetic Cost of Neanderthal Introgression. *Genetics* **203**, 881–891 (2016). doi: 10.1534/genetics.116.186890; pmid: 27038113
50. I. Juric, S. Aeschbacher, G. Coop, The Strength of Selection against Neanderthal Introgression. *PLOS Genet.* **12**, e1006340 (2016). doi: 10.1371/journal.pgen.1006340; pmid: 27824859
51. M. A. Beaumont, B. Rannala, The Bayesian revolution in genetics. *Nat. Rev. Genet.* **5**, 251–261 (2004). doi: 10.1038/nrg1318; pmid: 15131649
52. M. A. Beaumont, Approximate Bayesian Computation. *Annu. Rev. Stat. Appl.* **6**, 379–403 (2019). doi: 10.1146/annurev-statistics-030718-105212
53. N. P. Cooke, S. Nakagome, Fine-tuning of Approximate Bayesian Computation for human population genomics. *Curr. Opin. Genet. Dev.* **53**, 60–69 (2018). doi: 10.1016/j.gde.2018.06.016; pmid: 30029009
54. J. K. Pritchard, M. T. Seielstad, A. Perez-Lezaun, M. W. Feldman, Population growth of human Y chromosomes: A study of Y chromosome microsatellites. *Mol. Biol. Evol.* **16**, 1791–1798 (1999). doi: 10.1093/oxfordjournals.molbev.a026091; pmid: 10605120
55. M. A. Beaumont, W. Zhang, D. J. Balding, Approximate Bayesian computation in population genetics. *Genetics* **162**, 2025–2035 (2002). doi: 10.1093/genetics/162.4.2025; pmid: 12524368
56. D. N. Harris *et al*., Diverse African genomes reveal selection on ancient modern human introgressions in Neanderthals. *Curr. Biol.* **33**, 4905–4916.e5 (2023). doi: 10.1016/j.cub.2023.09.066; pmid: 37837965
57. J.-J. Hublin *et al*., New fossils from Jebel Irhoud, Morocco and the pan-African origin of *Homo sapiens*. *Nature* **546**, 289–292 (2017). doi: 10.1038/nature22336; pmid: 28593953
58. E. M. L. Scerri *et al*., Did Our Species Evolve in Subdivided Populations across Africa, and Why Does It Matter? *Trends Ecol. Evol.* **33**, 582–594 (2018). doi: 10.1016/j.tree.2018.05.005; pmid: 30007846
59. D. Richter *et al*., The age of the hominin fossils from Jebel Irhoud, Morocco, and the origins of the Middle Stone Age. *Nature* **546**, 293–296 (2017). doi: 10.1038/nature22335; pmid: 28593967
60. C. Stringer, J. Galway-Witham, On the origin of our species. *Nature* **546**, 212–214 (2017). doi: 10.1038/546212a; pmid: 28593955
61. C. M. Vidal *et al*., Age of the oldest known *Homo sapiens* from eastern Africa. *Nature* **601**, 579–583 (2022). doi: 10.1038/s41586-021-04275-8; pmid: 35022610
62. K. Harvati *et al*., Apidima Cave fossils provide earliest evidence of *Homo sapiens* in Eurasia. *Nature* **571**, 500–504 (2019). doi: 10.1038/s41586-019-1376-z; pmid: 31292546
63. I. Hershkovitz *et al*., The earliest modern humans outside Africa. *Science* **359**, 456–459 (2018). doi: 10.1126/science.aap8369; pmid: 29371468
64. C. Stringer, J. Galway-Witham, When did modern humans leave Africa? *Science* **359**, 389–390 (2018). doi: 10.1126/science.aas8954; pmid: 29371454
65. R. M. Beyer, M. Krapp, A. Eriksson, A. Manica, Climatic windows for human migration out of Africa in the past 300,000 years. *Nat. Commun.* **12**, 4889 (2021). doi: 10.1038/s41467-021-24779-1; pmid: 34429408
66. R. Grün *et al*., U-series and ESR analyses of bones and teeth relating to the human burials from Skhul. *J. Hum. Evol.* **49**, 316–334 (2005). doi: 10.1016/j.jhevol.2005.04.006; pmid: 15970310
67. H. S. Groucutt *et al*., *Homo sapiens* in Arabia by 85,000 years ago. *Nat. Ecol. Evol.* **2**, 800–809 (2018). doi: 10.1038/s41559-018-0518-2; pmid: 29632352
68. H. S. Groucutt *et al*., Multiple hominin dispersals into Southwest Asia over the past 400,000 years. *Nature* **597**, 376–380 (2021). doi: 10.1038/s41586-021-03863-y; pmid: 34471286
69. L. Slimak *et al*., Modern human incursion into Neanderthal territories 54,000 years ago at Mandrin, France. *Sci. Adv.* **8**, eabj9496 (2022). doi: 10.1126/sciadv.abj9496; pmid: 35138885
70. S. Peyrégne, J. Kelso, B. M. Peter, S. Pääbo, The evolutionary history of human spindle genes includes back-and-forth gene

flow with Neandertals. *eLife* **11**, e75464 (2022). doi: 10.7554/eLife.75464; pmid: 35816093
71. M. Petr *et al*., The evolutionary history of Neanderthal and Denisovan Y chromosomes. *Science* **369**, 1653–1656 (2020). doi: 10.1126/science.abb6460; pmid: 32973032
72. C. Posth *et al*., Deeply divergent archaic mitochondrial genome provides lower time boundary for African gene flow into Neanderthals. *Nat. Commun.* **8**, 16046 (2017). doi: 10.1038/ncomms16046; pmid: 28675384
73. Q. Fu *et al*., An early modern human from Romania with a recent Neanderthal ancestor. *Nature* **524**, 216–219 (2015). doi: 10.1038/nature14558; pmid: 26098372
74. M. Hajdinjak *et al*., Initial Upper Palaeolithic humans in Europe had recent Neanderthal ancestry. *Nature* **592**, 253–257 (2021). doi: 10.1038/s41586-021-03335-3; pmid: 33828320
75. C. Stringer, L. Crété, Mapping Interactions of *H. neanderthalensis* and *Homo sapiens* from the Fossil and Genetic Records. *Paleoanthropology* **2022**, 401–412 (2022). doi: 10.48738/2022.iss2.130
76. F. H. Smith, I. Janković, I. Karavanić, The assimilation model, modern human origins in Europe, and the extinction of Neandertals. *Quat. Int.* **137**, 7–19 (2005). doi: 10.1016/j.quaint.2004.11.016
77. C. Lalueza-Fox, Neanderthal assimilation? *Nat. Ecol. Evol.* **5**, 711–712 (2021). doi: 10.1038/s41559-021-01421-3; pmid: 33828250
78. L. Chen, A. B. Wolf, W. Fu, L. Li, J. M. Akey, IBDmix: Identifying and Interpreting Apparent Neanderthal Ancestry in African Individuals, Source Code, *Code Ocean* (2021); doi: 10.24433/CO.5781869.v1
79. L. Li, T. Comi, R. Bierman, J. Akey, IBDmix calls of introgressed Neanderthal sequences in individuals from the 1000 Genomics Project populations, Data set, *Zenodo* (2024); doi: 10.5281/zenodo.10578630

ACKNOWLEDGMENTS

We thank members of the Akey laboratory for helpful feedback related to this work, especially S. Moon, A. B. Wolf, K. Zhang, D. Tagore, and H. Xu. We thank F. Mafessoni from the Max Planck Institute for Evolutionary Anthropology and K. Prüfer from the Max Planck Institute for the Science of Human History for discussing analyses related to demographic history. We also thank B. Vernot from the Max Planck Institute for Evolutionary Anthropology for providing S* call sets of Altai and Vindija. The computational work described here was performed using the Princeton Research Computing resources at Princeton University, which is a consortium of groups led by the Princeton Institute for Computational Science and Engineering (PICSciE) and the Office of Information Technology's Research Computing. **Funding:** This study was supported by National Institutes of Health grant R01GM110068 (J.M.A.). **Author contributions:** Conceptualization: J.M.A. and L.L. Methodology: J.M.A. and L.L. Investigation: J.M.A., L.L., T.J.C., and R.F.B. Visualization: J.M.A. and L.L. Funding acquisition: J.M.A. Project administration: J.M.A. Supervision: J.M.A. Writing – original draft: J.M.A. and L.L. Writing – review & editing: J.M.A., L.L., T.J.C., and R.F.B. **Competing interests:** The authors declare that they have no competing interests. **Data and materials availability:** IBDmix software is publicly available at https://github.com/PrincetonUniversity/IBDmix and Code Ocean (*78*). The introgressed Neanderthal sequences identified by IBDmix and the script to identify the genetic distance of IBDmix segments are publicly available at Zenodo (*79*).

SUPPLEMENTARY MATERIALS

science.org/doi/10.1126/science.adi1768
Materials and Methods
Figs. S1 to S18
Tables S1 to S12
References (*80*–*94*)
MDAR Reproducibility Checklist

Submitted 5 July 2023; accepted 14 May 2024
10.1126/science.adi1768